LPC CAEN

LABORATOIRE DE PHYSIQUE CORPUSCULAIRE

ISMRA - Boulevard Maréchal Juin - 14050 CAEN CEDEX - FRANCE

Thermodynamical equilibrium up to the gas phase?

F. Guilminelli, B. Borderie, D. Durand, Ma Y.G., J. Péter, M. F. Rivet, A. Siwek, M. Assenard, G. Auger, Ch. O. Bacri, E. Bisquer, R. Bougault, R. Brou, J.L. Charvet, A. Chbihi, J. Colin, D. Cussol, R. Dayras, E. De Filippo, A. Demeyer, D. Doré, P. Eudes, M. Germain, D. Guinet, P. Lautesse, J.L. Laville, J.F. Lecolley, A. Le Fèvre, T. Lefort, R. Legrain, O. Lopez, M. Louvel, V. Métivier, L. Nalpas, A. Ouatzerga, M.Parlog, E. Plagnol, A. Rahmani, T. Reposeur, E. Rosato, F. Saint-Laurent, M. Squalli, J.C. Steckmeyer B. Tamain, L. Tassan-Got, E. Vient, C. Volant, J.P. Wieleczko

Avril 1997

LPCC 97-07
IPNO-DRE 97 15
GANIL P 9714
CEA/DAPNIA/SPhN 97-25
LYCEN/ 9715
SUBATECH-97-

Invited talk to the XXXV Int. Winter Meeting
on Nuclear Physics Bormio (Italy), February 3-7, 1997

INSTITUT NATIONAL
DE PHYSIQUE NUCLEAIRE ET DE PHYSIQUE DES PARTICULES

CENTRE NATIONAL DE LA RECHERCHE SCIENTIFIQUE

INSTITUT DES SCIENCES
DE LA MATIERE ET DU RAYONNEMENT

Téléphone : 02 31 45 25 00
Télécopie : 02 31 45 25 49

THERMODYNAMICAL EQUILIBRIUM UP TO THE GAS PHASE ?

Francesca Gulminelli

LPC Caen, IN2P3-CNRS, ISMRA et Université , F-14050 Caen Cedex, France

and the INDRA Collaboration

[a]B. Borderie, [b]D. Durand, [b]Ma Y.-G. [1], [b]J. Péter, [a]M.F. Rivet, [b]A. Siwek [2], [f]M. Assenard, [c]G. Auger, [a]Ch.O. Bacri, [d]E. Bisquer, [b]R. Bougault, [b]R. Brou, [e]J.L. Charvet, [c]A. Chbihi, [b]J. Colin, [b]D. Cussol, [e]R. Dayras, [e]E. De Filippo, [d]A. Demeyer, [a]D. Doré, [f]P. Eudes, [f]M. Germain, [d]D. Guinet, [d]P. Lautesse, [f]J.L. Laville, [b]J.F. Lecolley, [c]A. Le Fèvre, [b]T. Lefort, [e]R. Legrain, [b]O. Lopez, [b]M. Louvel, [f]V. Métivier, [e]L. Nalpas, [a]A. Ouatizerga, [a]M. Parlog, [a]E. Plagnol, [f]A. Rahmani, [f]T. Reposeur, [b]E. Rosato, [c]F. Saint-Laurent, [a]M. Squalli, [b]J.C. Steckmeyer, [b]B. Tamain, [a]L. Tassan-Got, [b]E. Vient, [e]C. Volant, [c]J.P. Wieleczko

[a]*IPN Orsay (IN2P3-CNRS), F-91406 Orsay cédex, France*
[b]*LPC Caen (IN2P3-CNRS/ISMRA et Université), F-14050 Caen cédex, France*
[c]*GANIL (DSM-CEA/IN2P3-CNRS), B.P.5027, F-14021 Caen cédex, France*
[d]*IPN Lyon (IN2P3-CNRS/Université), F-69622 Villeurbanne cédex, France*
[e]*CEA DAPNIA-SPhN, CE Saclay, F-91191 Gif sur Yvette cédex, France*
[f]*SUBATECH (IN2P3-CNRS/Université), F-44072 Nantes cédex 03, France*

Abstract

A quantum statistical model including a final state excluded volume interaction is presented and thoroughly compared to the deexcitation of the Ar quasi-projectile measured by the INDRA collaboration in the Ar+Ni reaction at 95 A.MeV beam energy. At excitation energies greater than roughly 10 A.MeV the kinetic energies, first and second order moments of the multiplicity distributions and apparent temperatures can be consistently explained in terms of an equilibrated supercritical nuclear gas.

[1]on leave of absence from Institute of Nuclear Research, Shanghai, China.
[2]on leave of absence from Instytut Fizyki Jadrowej, Cracow, Poland.

1 Introduction

With the increasing availability of quasi complete and exclusive data on the deexcitation of well identified single nuclear sources in heavy ion reactions [1], the longstanding challenge of studying nuclear thermodynamics is finally becoming a concrete possibility. The experimental evidences of a complete memory loss of the entrance channel [1] and the satisfactory comparison with statistical models based on thermodynamical equilibrium [2] suggest that in a wide range of incident energies and impact parameters the dynamical and thermodynamical components may actually be decoupled, and that the application of physical concepts borrowed from macroscopic statistical mechanics, like thermal equilibrium, phase coexistence and phase transition, may be appropriate. In order to study nuclear thermodynamics one needs to be able to univocally associate the detected reaction products with the thermodynamical variables of the decaying source (temperature, density). In other words, a correct modelization of the temperature dependent partition function is needed to reconstruct the deexcitation chain and discriminate between prompt and secondary emission. At low excitation energies this aim is accomplished by the theory of compound nucleus. At higher excitation energies the opening of multifragmentation channels makes an exact evaluation increasingly difficult. Sophisticated Monte Carlo calculations of the multifragmentation pattern have been available for many years [2], but the internal partition function at high temperature is poorly known, and the suppression procedure of the state-density integral at high excitation energy is not unique. If we limit our attention to light fragments without states in the continuum, we expect that at high temperature the high lying discrete levels will be increasingly excited. Since most of these states are particle unstable, their population can significantly modify the light particle yields and energy spectra. Another difficulty raises from the fact that in statistical model calculations the assumption is commonly taken that the multifragmentation pattern can be calculated in a non interacting freeze out configuration. However, even in the framework of thermodynamical equilibrium, final state interactions at freeze out can modify the production yields [3]. The problem is simplified by the fact that the high lying resonances [4, 5] and a thermodynamically consistent interaction [6, 5] are straightforwardly included in the macrocanonical partition function, and at a temperature of the order

of the critical temperature the macrocanonical and microcanonical descriptions are completely equivalent [2].

An experimental study on the quasi-projectile formed in Ar+Ni reactions in the range 52-95 A.Mev bombarding energy has recently shown [7, 8] that in these binary reactions isotropically decaying sources can be formed with an excitation energy up to 28 MeV per nucleon. The decay pattern is independent of the incident energy and the kinetic energy spectra of the different fragments have a Boltzmann shape with approximately the same slope, thus suggesting an equilibrated disintegration even at excitation energies which would correspond to temperatures above the critical temperature for finite nuclei [9].

The purpose of this paper is to trace back the formation of such a supercritical gas by comparing the data to a simple model of thermodynamical equilibrium which includes feeding from discrete and continuum states and a first order density correction in the freeze out equation of state [5].

2 Chemical and Thermal Equilibrium Fireball Model

The physical scenario we have in mind is a chemically and thermally equilibrated nuclear source which undergoes a simultaneous disassembly at a fixed temperature T and density ρ [10]. For a number K of different quantum non interacting structureless species inside a volume V, the entropy reads

$$S_0 = -V \sum_{i=1}^{K} \frac{g_i}{h^3} \int d^3p \, n_i(\vec{p}) \, log \, n_i(\vec{p}) \pm \Big(1 \mp n_i(\vec{p})\Big) log\Big(1 \mp n_i(\vec{p})\Big) \qquad (1)$$

where n_i is the occupation of each energy state, g_i is the degeneracy factor and the upper (lower) sign accounts for Fermi (Bose) statistics. The free energy is defined as usual as

$$F = E - TS = V \sum_{i=1}^{K} \frac{g_i}{h^3} \int d^3p \Big(E_i + \frac{p^2}{2m_i}\Big) n_i(\vec{p}) - TS \qquad (2)$$

in which E_i represents the energy of the considered state. Thermal equilibrium in the macrocanonical ensemble implies the definition of a chemical potential as

$$\frac{h^3}{g_i} \frac{\partial F}{\partial n_i} = \mu_i \qquad (3)$$

The multiplicity of each species then results [4, 11]

$$M_i = \frac{V g_i \left(m_i T\right)^{3/2}}{\sqrt{2}\pi^2\hbar^3} \int_0^\infty dz\sqrt{z}\Big(exp(z - \frac{\mu_i}{T} + \frac{E_i}{T}) \pm 1\Big)^{-1} \tag{4}$$

where the sum runs over the ground state and excited states of the different isotopes. The mass action law of chemical equilibrium implies for the chemical potential of the i-th species

$$\mu_i = \mu_Z Z_i + \mu_N N_i \tag{5}$$

Here, Z_i and N_i are the atomic and neutron number of species i and μ_N (μ_Z) are the neutron (proton) constant chemical potentials, to be determined at any given density to ensure conservation of the total neutron and proton number N, Z

$$N = \sum_{i=1}^{K} N_i \, M_i \left(\mu_i, T\right) \tag{6}$$

$$Z = \sum_{i=1}^{K} Z_i \, M_i \left(\mu_i, T\right) \tag{7}$$

The freeze out (or break up) density is calculated by [12]

$$\rho_{\mathrm{FO}} = \frac{N+Z}{V_{\mathrm{FO}}} = \frac{N+Z}{V + \sum_{i=1}^{K} V_i M_i} \tag{8}$$

where V_i represents the proper volume of the species i. In this formalism the discrete levels of the different isotopes at an excitation energy E_i^* are treated as independent structureless particles characterized by an internal energy augmented with respect to the ground state binding energy B_i as $E_i = B_i + E_i^*$, and by their proper degeneracy factor g_i. This corresponds to the implicit assumption that these states are sufficiently narrow, *i.e.* their life time is much longer than the equilibration time. In this work all known discrete levels of nuclear species with $Z \leq 10$ and width Γ less than a cut-off value Γ_0 are included in the state sum [13], and continuum states are allowed for nuclei of $10 \leq Z \leq 20$ in the form of an effective Fermi gas level density [14]

$$\rho_{\mathrm{FG}} \left(\epsilon\right) = kA^{-p} exp(2\sqrt{a\left(A\right)\epsilon}) exp(-\epsilon/T_0\left(A\right)) \tag{9}$$

where the parameters are taken from ref.[14] and the limiting temperature T_0 is related for any mass number A to the cut off width Γ_0 by Weisskopf theory [15] through the life time τ of the decaying system. Since τ is for any Γ_0 much shorter

than the time of flight towards the detector, the populated excited states are made subsequently decay with the experimentally known branching ratios when available [13], and Weisskopf theory otherwise.

Let us now turn to the problem of final state interactions. We have already remarked that in the model proposed above the nuclear gas is completely ideal, *i.e.* the different species do not interact. For this to be true, the freeze out volume must be considerably larger than the proper volume of the particles. One possible method of dealing with collisions and reabsorption at freeze out is given by an effective excluded volume approach in the spirit of the Van der Waals gas. This method is issued from atomic physics, where it is well known that the partition function diverges if all the states are included in the thermodynamical potential [16]. This artificial divergence comes from the highly unbound excited states which are characterized by orbitals of increasing dimensions and therefore are absorbed by the interaction with neighboring atoms. In an analogous way, the loosely bound particle unstable resonances with a density distribution extending far off the liquid drop mean square radius have to be suppressed from the count of states if the inter-particle distance is smaller than the range of their wave function [10, 17].
In the framework of the effective Van Der Waals formalism, the entropy of a non ideal gas at the first order in the density is given by

$$S = S_0 + n\,log\Big(1 - \frac{b}{V}\Big) \tag{10}$$

where S_0 is the ideal gas limit given by equation (1), and b is related to the proper volume of the components through

$$b = \frac{1}{2n}\sum_{i,j}^{K} M_i M_j (V_i^{1/3} + V_j^{1/3})^3 \tag{11}$$

where n is the total multiplicity and V_i is the proper volume of the i-th species. The population of each species then gets a density dependent correction

$$M_i = \frac{g_i\,(m_i T)^{3/2}}{\sqrt{2}\pi^2\hbar^3}\int_0^\infty dz\sqrt{z}\Big(exp(z - \frac{\mu_i}{T} + \frac{E_i}{T} + f_i) \pm 1\Big)^{-1} \tag{12}$$

with a suppression factor which is more important the "bigger" the particle is

$$f_i = \frac{n}{V}\frac{\partial b}{\partial M_i} = \sum_{j=1}^{K}\frac{M_j}{V}(V_i^{1/3} + V_j^{1/3})^3 \tag{13}$$

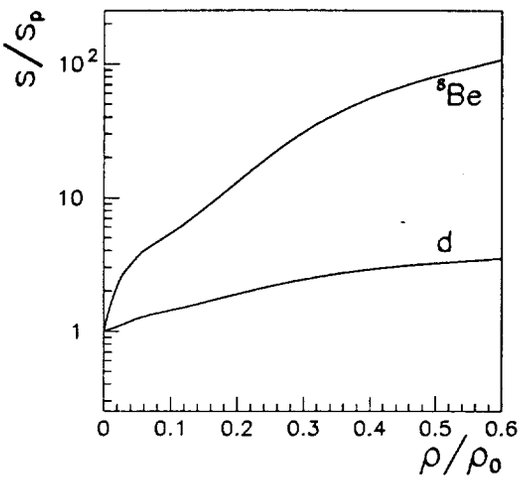

Figure 1: Suppression factor (see text) for deuterons and ^8Be as a function of the freeze out density for a fixed $T = 10$ MeV temperature.

For any fixed value of temperature and chemical potentials, eq.(12) is iteratively solved for the freeze out volume up to convergence. For the volumes V_i we have taken a spherical shape from the experimental mean square radius for the ground states, and for the resonant structures we have made the hypothesis that the exit channel is preformed in the decaying state. There are some theoretical studies supporting this picture, in particular for species with strong alpha decaying channels [18]. Thus for example a ^8Be will be parametrized as two adjacent alpha particles [19], corresponding to an effective spherical volume entering in the final state interaction with a radius equal to twice the alpha particle radius. Of course this is a very simplistic representation which has to be viewed only as a first attempt to incorporate a mean nuclear interaction in the freeze out configuration.

The effect of the excluded volume interaction is to favour protons, neutrons and alphas over the more loosely bound structures like deuterons and high lying resonances. This is shown in figure 1, which displays the suppression factor $s_i = exp(f_i)$ of eq.(13) for deuterons and ^8Be normalized to the s_p of a proton as a function of the break up density. One can see that the source is behaving as an ideal gas only in the limit of vanishing density.

3 Comparison to Vaporization Data

As a first application we shall compare the model to a specific class of events detected in the Ar+Ni reaction by the INDRA collaboration [8], where no reaction product has an atomic number greater than 2 ("vaporization" events). For such

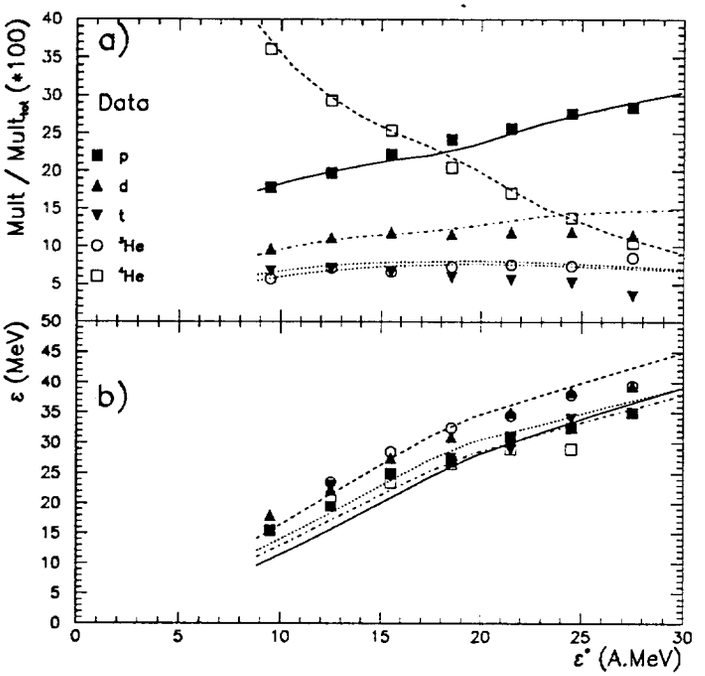

Figure 2: Relative multiplicity of light charged particles (fig.2a) and average kinetic energies (fig.2b) as a function of excitation energy for vaporization events in the quasi-projectile deexcitation from the reaction $Ar + Ni$ at 95 MeV/u. Symbols: experimental data from ref.8. Lines: calculation. Full lines: protons, dashed lines: alphas, dashed dotted lines: deuterons, dotted lines: tritons and ^3He.

events the energy detection thresholds are virtually irrelevant, the isotopes are fully resolved and the detection is complete except from the neutrons which however can be obtained from mass conservation with a minimum bias approximation due to the small size of the system. Apart from the completeness of the information, these events are interesting because they represent an extreme deexcitation mode for a hot nucleus, close to the intuitive expectation of a supercritical nuclear gas as a

system composed of only free nucleons. Vaporization events, which are involved in binary dissipative collisions, correspond to a cross section of the order of some tens of microbarns, which becomes significant with respect to the total detected cross section only at the highest excitation energies measured [8]. Let us focus now on the quasi-projectile. In the thermodynamical model presented in the last section only average quantities can be computed. Therefore for a comparison to the data one has to calculate conditional distributions, under the constraint that the "vaporization" condition $Z \leq 2$ is satisfied. This amounts to include in the partition function only the states which, after decay, give no particle heavier than an α-particle. The result [5] of the calculation for the average multiplicities and kinetic energies is shown in figure 2 as a function of excitation energy, compared to experimental data [8]. Apart from small deviations in the kinetic energies, the reproduction is very satisfactory. In this calculation the freeze out density has been fixed to one third of the saturation density, the cut-off width of resonances is $\Gamma_0 = 2$ MeV, and the excluded volume interaction is included. In order to obtain this degree of agreement to the data the interaction is very important. In the ideal gas case, the experimental proton over deuteron ratio can be fitted only by imposing a freeze out density so low that the proton over alpha ratio is overestimated by more than an order of magnitude [5]. In this calculation as in the following ones the (average) excitation energy is univocally defined for any input temperature and density as

$$E^* = < E > - B_s = \sum_i M_i(T_i + B_i + V_i) - B_s \qquad (14)$$

where T_i is the average kinetic energy of the $i-$th species, V_i is the average inter-particle Coulomb energy assumed independent of the freeze out configuration [20], and B_s is the binding energy of the source. Figure 3 shows the sensitivity of the relative multiplicities and of the average kinetic energies to the cut-off parameter employed. Secondary decays contribute especially to the alpha and proton yields, but the influence of the parameter Γ_0 is almost within the experimental error bars. The slight but systematic overestimation of the alpha kinetic energies observed in figure 2 seems to indicate that the resonant yield is relatively low, since figure 3 shows that secondary decays tend to increase the average energy of alpha particles. This last remark does not mean that side feeding effects from particle decaying states can be neglected. Even with the suppression effect of the excluded volume inter-

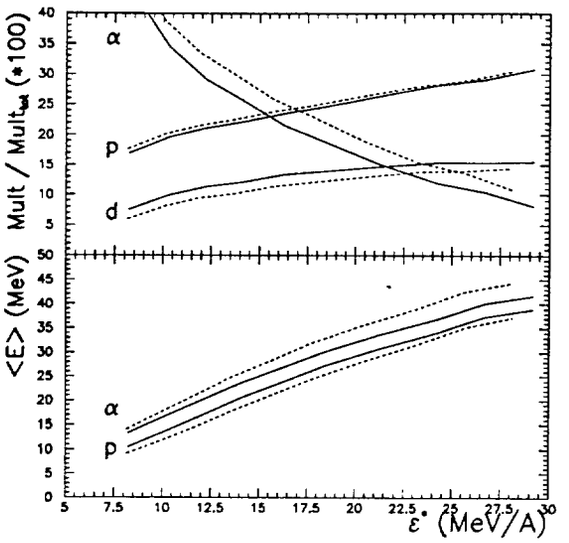

Figure 3: Effect of the Γ_0 parameter on the calculated multiplicities (upper panel) and energies (lower panel) of the particles. Full lines: $\Gamma_0 = 1$ MeV. Dashed lines: all non broad states included.

action and with a very low Γ_0 parameter side feeding plays a very important role especially on alpha particles. This is shown in figure 4 which displays the prompt and secondary contribution to the alpha and proton spectra at an excitation energy of 16 A.MeV: the majority of alphas come from secondary decays. The last parameter to be discussed is the freeze-out density, which is the only critical parameter of the model. A change in the density only very slightly affects the kinetic energies, but produces a sizeable modification in the production yields as it is shown in figure 5. Protons and deuterons are increasingly favoured over alphas as the density decreases. Since no principle reason can be invoked to choose the density within 20% or even 50%, other observables independent of the mean multiplicities have to be considered before one can convincingly state that thermodynamical equilibrium has been reached. To this aim we have compared the second moments of the distributions, namely the variances in the particle multiplicities. In principle variances can be analytically calculated as well as mean values in the macrocanonical ensemble. These variances originate from the random exchanges of particles and energy with the thermal bath. However it is experimentally observed [8] that no thermal equilib-

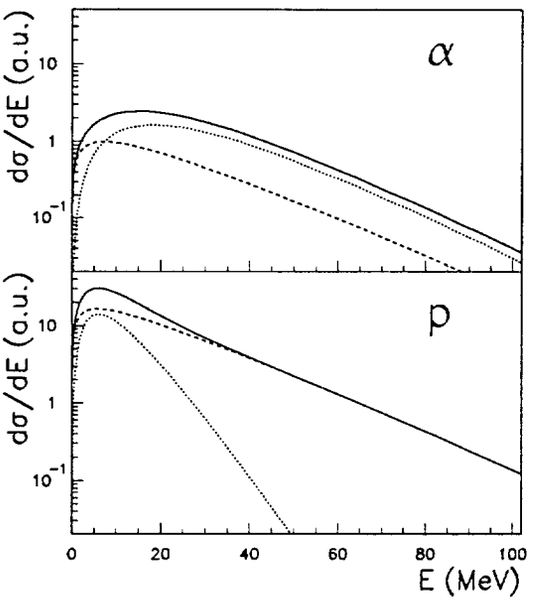

Figure 4: Alpha (upper panel) and proton (lower panel) kinetic energy spectrum calculated with $\Gamma_0 = 1$ MeV at an excitation energy of 16 A.MeV. Full lines: total yield. Dashed lines: prompt emission. Dotted lines: secondary decays.

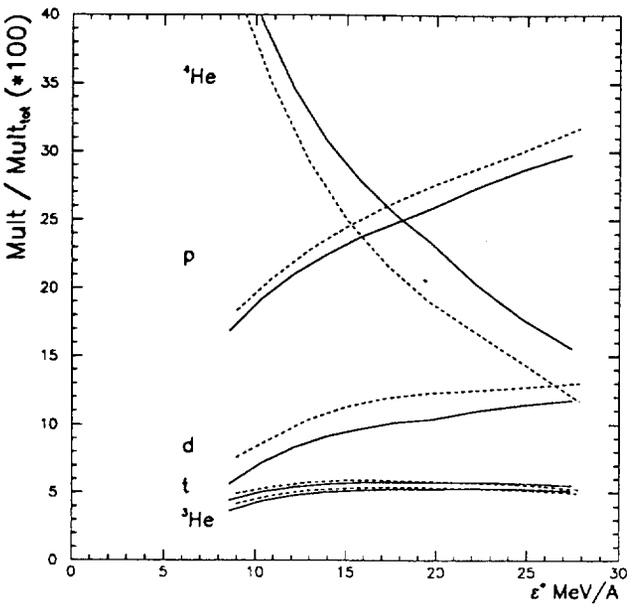

Figure 5: Relative particle multiplicities as a function of excitation energy calculated at a freeze out density $\rho = 0.045$ fm^{-3} (solid lines) and $\rho = 0.035$ fm^{-3} (dashed lines)

rium is achieved between the two reaction partners, due to the short reaction time. This means that the quasi-target cannot be considered as a thermal bath for the quasi-projectile, and that the observed fluctuations in mass and excitation energy of the source have a dynamical origin. Therefore the variances of the multiplicities will have, together with a thermal component, a non equilibrated contribution coming from the mass and energy fluctuations of the entrance channel. In order to get rid of this non-equilibrium component, the width of the measured mass and excitation energy distribution of the source has been used as an input of the statistical calculation. A Monte Carlo simulation allows to generate events from the macrocanonical probabilities, with a distribution of temperatures such as to cover the experimental excitation energy range, and a source mass and excitation energy distribution fitted from the data. The result [21] of this simulation is reported in figure 6. The order of magnitude is correctly reproduced, as well as the behaviour of the curves as a function of excitation energy. The thermal origin of the observed fluctuations is confirmed by a simulation (dashed curves) where, at each excitation energy, the

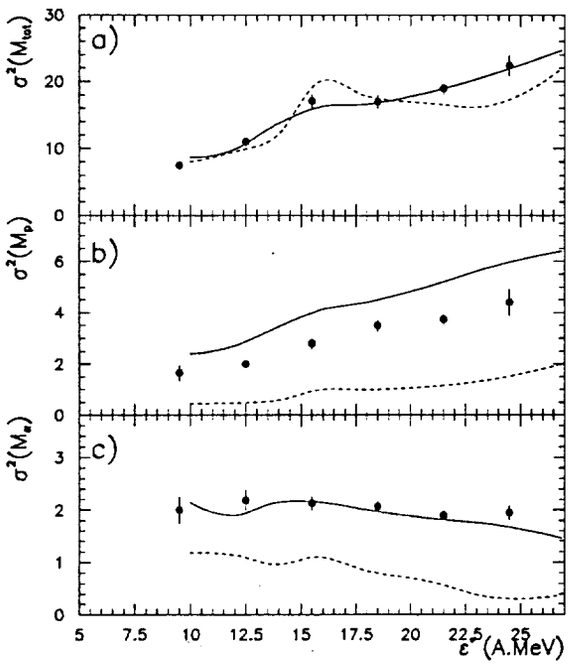

Figure 6: Second moment of the total (fig.6a), proton (fig.6b) and alpha (fig.6c) multiplicity distribution as a function of excitation energy. Symbols: experimental data. Full lines: Montecarlo simulation. Dashed lines: entrance channel fluctuations (see text).

statistical fluctuations are frozen (i.e. the partitions are fixed) and only the source mass is allowed to vary with a width fixed by the experimental distribution. The resulting fluctuations are insufficient to explain the variations observed.

4 The High Energy Branch of the Nuclear Caloric Curve

A longstanding challenge in nuclear physics is the possibility of observing a liquid-gas phase transition. To this aim the functional relationship between temperature and excitation energy (the so called caloric curve) has been studied at lenghth by different collaborations on different decaying systems [22, 23, 7]. The Aladin collaboration [22] observes a plateau followed by a linear rise starting at about 10 A.MeV excitation energy which is interpreted as a coexistence phase followed by a vapour phase. The plateau is not observed by the INDRA [7] and EOS [23] collaborations. The problem is complicated by the fact that temperature is not a direct observable in nuclear physics. Different thermometers have been proposed to study nuclear thermodynamics, namely slopes of light particle kinetic energy spectra (T_s) [24], relative populations of excited states (T_{ex}) [25], double ratios of multiplicities of neighbour isotopes (T_{iso}) [26] like the $(^6Li/^7Li)/(^3He/^4He)$ thermometer used by ALADIN (hereby abbreviated as He/Li), and the different thermometers can give, for the same excitation energy, very different results. A striking example is given by the INDRA data for the Ar+Ni system [7], where at the highest excitation energy the measured temperature can vary from 2 to 20 MeV depending on the thermometer employed. Dynamical effects can be invoked to explain this feature [27, 28]; since the temperature of the system is most likely a time depending variable, the different thermometers may reflect different stages of the reaction, thus making the experimental detection of a liquid-gas phase transition difficult if not impossible. On the other side in the framework of thermodynamical equilibrium, as we have seen in the preceding section, both side feeding and the final state interaction affect strongly particle multiplicities and kinetic energy spectra, thus deforming the response of the thermometers. Since the results of the previous section suggest that statistical models can give a very good description of the deexcitation even in the extreme case of a

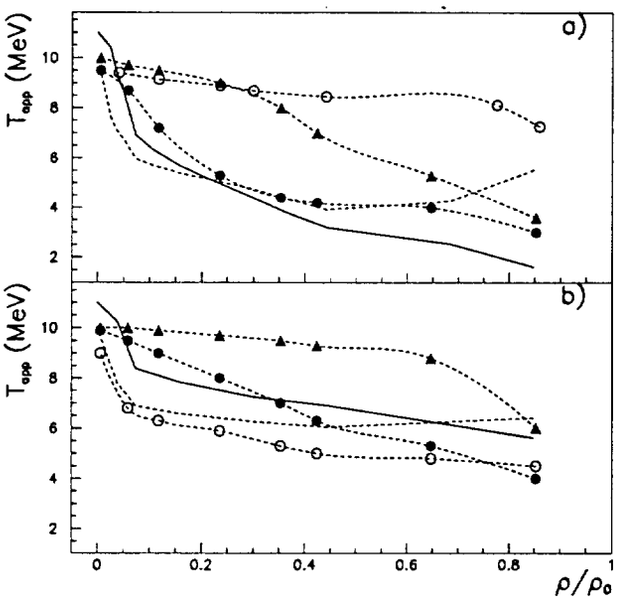

Figure 7: Calculated apparent temperatures without (7a) and with (7b) excluded volume interaction as a function of the freeze out density. The thermodynamical temperature is 10 MeV. The mass number of the decaying source is $A = 100$ and the cut-off parameter is $\Gamma_0 = 2$ MeV. Line with open circles: temperature extracted from the population ratio of the ground state and excited state ($E^* = 16.66$ MeV) of ^5Li. Lines: temperatures from double ratios of neighbour isotopes (Full:$(^6Li/^7Li)/(^3He/^4He)$. Dashed:$(d/t)/(^3He/^4He)$). Lines with full symbols: temperatures from the slope of light particle spectra (circles: protons, triangles: deuterons).

vaporized source, it is challenging to explore the possibility that the whole set of the INDRA data at high excitation energy can be explained in terms of a supercritical equilibrated gas [5]. In this section we shall therefore compute within the model the different caloric curves than have been measured with the different thermometers. As we have already seen, the critical parameter of the calculation is the freeze out density. Both side feeding and the excluded volume interaction depend on density in a strong and highly non linear way. The effect on the thermometers is shown in figure 7 which gives the response of different kinetic, excited states, and isotopic thermometers to the same $T = 10$ MeV thermodynamical temperature, as a function of the freeze out density. Some systematic trends can be seen: in the ideal gas case the best thermometer is represented by the excited states population ratio, since only a few resonances have a non zero branching ratio to ^5Li. Deuteron slopes apparent temperature are closer to the thermodynamical temperature than proton ones, again because side feeding affects protons more than deuterons. On the other side the excluded volume interaction suppresses the high lying resonances, thus reducing the effect of secondary decays on particle slopes and reducing the value of the apparent temperatures based on populations of excited states. From figure 7 we can conclude that a precise knowledge of the freeze out density is indispensable if we want to quantitatively calculate the response of the different thermometers [29, 30]. As it is stressed in ref.[29], it is very important to fix the parameters of the model in order to reproduce the experimental mass distribution, a too steep distribution resulting in an underprediction of secondary feeding corrections. We have therefore chosen to fix the freeze out density in order to reproduce, at any temperature, the experimental ratio $Z_{\rm LCP}/Z_{\rm tot}$ between the charge stored in light charged particles ($Z \leq 2$) and the total source charge, which is a direct measure of the observed vapour over liquid population. The liquid over vapour fraction is itself linked, through the value of the chemical potential, to the freeze out density. The clear correlation of this variable to the freeze out density is demonstrated in figure 8. Non crossing and smoothly varying isothermal lines are obtained by varying the break up density over a wide range, thus allowing to associate to any excitation energy an unique value of temperature and chemical potential. We have chosen to constrain the calculation with this variable, rather than with the complete charge distribution, since finite size

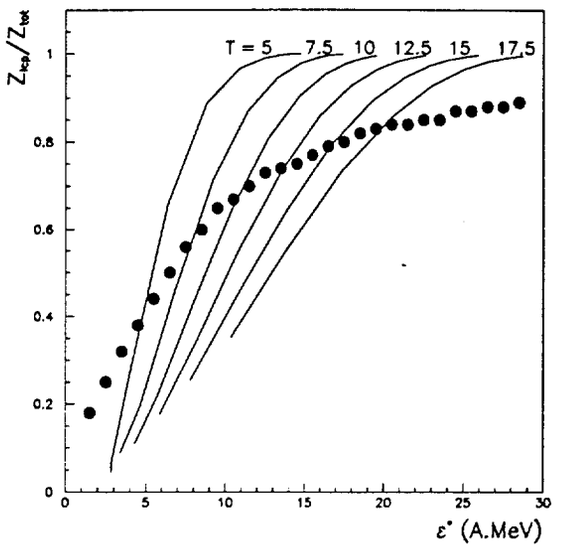

Figure 8: Isothermal lines in the $Z_{\rm LCP}/Z_{\rm tot}$ versus excitation energy plane for a decaying source with a mass $A = 36$. Increasing density goes in the direction of decreasing energy. Symbols: experimental data from ref.7.

effects (which are treated in an oversimplified way in this macrocanonical model) are expected to influence mostly the production of fragments with a size comparable to the size of the system. The charge distributions for different excitation energy bins are compared to the predictions of the model in figure 9. In this figure one can see that, once $Z_{\rm LCP}/Z_{\rm tot}$ is fixed, the charge distributions are well reproduced for excitation energies larger than about 10 MeV per nucleon. At lower excitation energies the yields of fragments with $Z>10$ are systematically underestimated, suggesting that the picture of a loosely interacting nuclear gas is not valid in this excitation energy range. Figure 10 displays the result of the calculation with the excluded volume interaction for the different double ratios $T_{\rm iso}$'s, the deuteron T_s and the T_{exc} for ^5Li measured in the experiment [7, 31]. All the apparent temperatures are reasonably well reproduced, thus suggesting that collective effects play a minor role and thermodynamical equilibrium can actually have been reached in this reaction. The initial temperature is very close to the deuteron slope parameter, while all the temperatures extracted from double ratios have important feeding corrections. Temperatures extracted from the excited states population ratios are affected by feeding

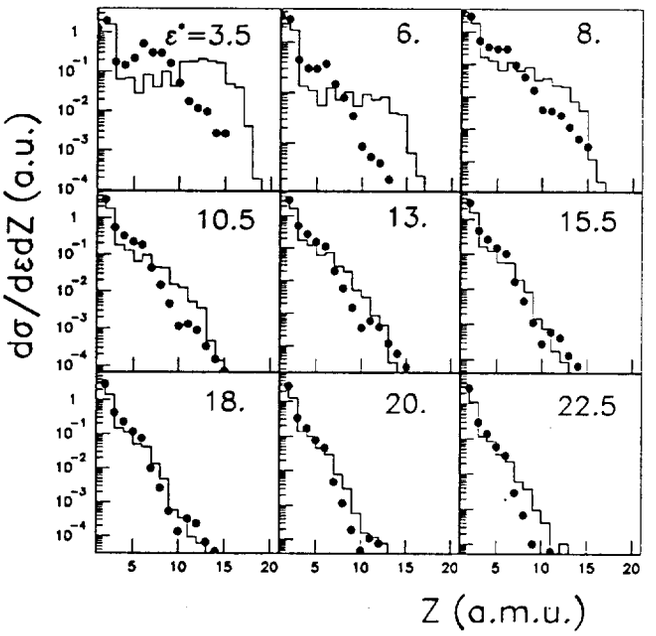

Figure 9: Calculated (full symbols) and experimental (histograms) charge distributions in different excitation energy bins for the quasi projectile formed in the Ar+Ni reaction at 95 A.MeV beam energy.

and, more important, by the suppression effect of the excluded volume interaction. Of course the numerical value of these temperatures is strongly dependent on the shape assumed for the discrete excited states. For example an arbitrary reduction of a factor two in the assumed volume of resonant states leads to an increase of about 1 MeV of the calculated value of T_{exc} for ^5Li. Here we just want to stress the qualitative idea that the low temperatures systematically extracted from excited state populations may be due to the suppression of the more loosely bound structures via a final state interaction. In the context of this model the slope parameter

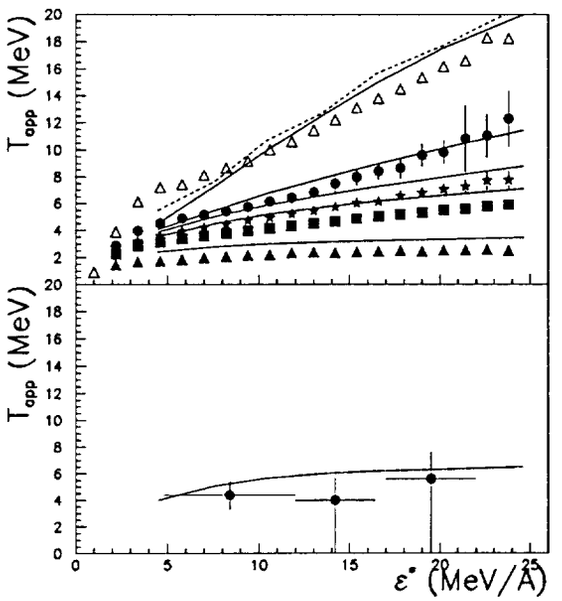

Figure 10: Apparent temperature as a function of excitation energy per nucleon. Symbols: experimental data from ref.7,30. Full lines: this model for a decaying $A = 36$ source and $\Gamma_0 = 2$ MeV. Dashed line: thermodynamical temperature used in the calculation. Upper part: deuteron slopes (open triangles) and different isotopic double ratios. Circles: $(^6Li/^7Li)/(^3He/^4He)$. Stars: $(d/t)/(^3He/^4He)$. Squares: $(p/d)/(^3He/^4He)$. Triangles: $(p/d)/(^6Li/^7Li)$ Lower part: temperature extracted from the population ratio of the ground state and excited state ($E^* = 16.66$ MeV) of ^5Li in the calculation and in the experiment.

appears as the most accurate thermometer. The calculation presented in figure 10

was performed with a cut-off parameter $\Gamma_0 = 2$ MeV. The slope parameter is unaffected by the value of Γ_0 while the He/Li isotopic temperature is decreased by increasing the number of resonances allowed in the calculation [5]. However for life times $\tau \leq 100$ fm/c ($\Gamma_0 \geq 2$) the result is not strongly dependent on this parameter, due to the resonance suppression effect of the excluded volume interaction [5]. As it was observed in ref.[7], for excitation energies lower than approximately 10 MeV per nucleon, the experimental apparent temperature extracted from deuteron slopes are compatible with a Fermi gas energy/temperature relation $T = \sqrt{aE^*}$. Neither in the data nor in the calculation a plateau is observed, but the failure of the model at low excitation energies suggests that we are facing a transition between an evaporative regime characterized by a Fermi gas density of states, and a multifragmentation one where the system can be described as a supercritical gas of loosely interacting nuclear species in thermodynamical equilibrium. In the context of the Berlin model [32], such a behaviour is characteristic of a first order phase transition. The effect

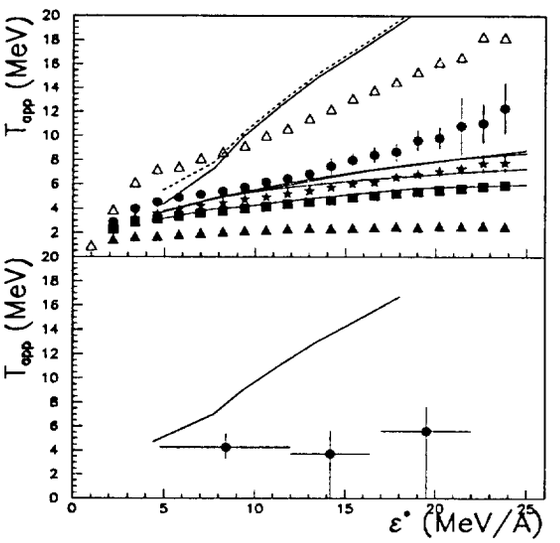

Figure 11: As figure 10 above, but without final state interaction and $\Gamma_0 = 1$ MeV.

of neglecting the correction to the ideal gas situation is dramatic, as it is shown in figure 11. The T_{ex} thermometer is overestimated, the experimentally observed difference between the isotopic thermometers is not reproduced, and the net effect of side feeding is augmented. Since most of the resonances have an important branching

ratio to alpha particle decay, in the ideal gas case side feeding effects are probably overestimated.

5 Conclusions

In this contribution we have presented an extended QSM model [5] which includes side feeding from continuum states and a schematic final state excluded volume interaction. We have applied the model to the deexcitation of the Ar quasi-projectile measured by the INDRA collaboration. All the observables measured in the va-

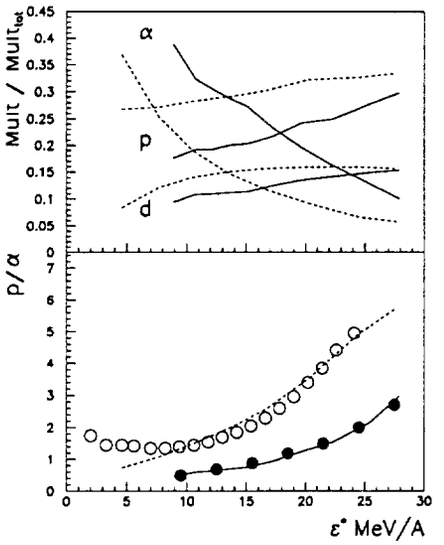

Figure 12: Upper part: relative alpha, proton and deuteron multiplicities as a function of excitation energy calculated with (full lines) and without (dashed lines) the vaporization condition. Lower part: proton over alpha multiplicity ratio as a function of excitation energy. Full symbols: vaporization data (ref.8). Open symbols: data for all events (ref.7). Lines as in the upper part.

porization events are fairly well reproduced by the model, suggesting that thermodynamical equilibrium has been reached in these reactions and dynamical effects play a minor role. No bias is introduced by restricting oneself to the vaporization events, as it is demonstrated in figure 12, which shows the effect on multiplicities of removing the vaporization constraint. Vaporization events are characterized by

an excess of alpha particles and become more representative of the whole production cross section as the excitation energy increases. This experimental observation comes in naturally in the model once the vaporization condition ($Z \leq 2$) is applied. The hypothesis of thermodynamical equilibrium is also compatible with the experimental measurement of different temperatures using different thermometers [7]. We have analyzed in detail the different origins of the biased response of the thermometers, side feeding and final state interactions playing a leading role. The model fails to reproduce the $Ar + Ni$ data at 95 MeV/u [7] for excitation energies lower than approximately 10 MeV/u, thus showing a clear transition from an evaporative regime to a multifragmentation one. In this regime, the data can be fairly well reproduced by the scenario of a quantum weakly interacting gas of nuclear species in thermodynamical equilibrium. This supercritical gas is characterised by a linear dependence of temperature as a function of excitation energy, differing however from the classical expectation $E^* = 3T/2$ because of its composite structure.

References

[1] N. Marie et al., Phys.Lett. B 391 (1997) 15, and references therein.

[2] D. H. E. Gross, Rep.Prog.Phys. 53 (1990) 605; J. Bondorf, A. S. Botvina, A. S. Iljinov, I. N. Mishustin and K. Sneppen, Phys.Rep.257 (1995) 133, and references therein.

[3] J. A. Lopez and J. Randrup, Nucl.Phys. A 503 (1989) 183.

[4] D. Hahn and H. Stoecker, Nucl.Phys. A 476A (1988) 719.

[5] F. Gulminelli and D. Durand, Nucl.Phys. A, in press.

[6] C. P. Singh, B. K. Patra and K. K. Singh, Phys.Lett. B 387 (1996) 680.

[7] Y. G. Ma et al, Phys.Lett. B 390 (1997) 41.

[8] M. F. Rivet et al., Phys. Lett. B 388 (1996) 219; B. Borderie et al.,Phys. Lett. B 388 (1996) 224.

[9] H. R. Jaqaman et al., Phys. Rev. C 29 (1984) 2067.

[10] A. Z. Mekjian, Phys.Rev. C 17 (1978) 1051; S. Das Gupta and A. Z. Mekjian, Phys.Rep. 72 (1981) 131.

[11] J. Konopka, H. Graf, H. Stoecker and W. Greiner, Phys.Rev. C 50 (1994) 2085.

[12] P. R. Subramanian et al., J.Phys. G 7 (1981) L241.

[13] J. Konopka, private communication; F. Ajzenberg-Selove, Nucl.Phys. A 320, 449, 475, 506, 521, 564 (1979-1993)

[14] S. E. Koonin, J. Randrup, Nucl. Phys. A 474 (1987) 173.

[15] V. Weisskopf, Phys. Rev. 52 (1937) 295.

[16] E. Fermi, Zeit. Phys. 26 (1924) 54.

[17] A.J. Cole, D. Heuer and M. Charvet, Phys. Rev. C, submitted.

[18] Proceedings of the Second International Conference on Atomic and Nuclear Cluster at Santorini, Z.Phys. A 349 (1994) 227-340.

[19] H.Horiuchi et al, Z.Phys. A 349(1994)279.

[20] J. Randrup and S. E. Koonin, Nucl.Phys. A 356 (1981) 223.

[21] B.Borderie et al., contribution to the International Workshop on Heavy Ion Physics at Low, Intermediate and Relativistic Energy with 4π Detectors, Poiana Brasov, Romania, (1996).

[22] J. Pochodzalla et al., Phys.Rev.Lett. 75 (1995) 1040.

[23] J. A. Hauger et al., Phys.Rev.Lett. 77 (1996) 235.

[24] R. W. Minich et al., Phys.Lett. B 118, (1982) 458; A. S. Hirsch et al., Phys.Rev. C 29 (1984) 508; R. Wada et al., Phys.Rev. C 39 (1989) 497; M. Gonin et al., Phys.Lett. B 217 (1989) 406; D. Cussol et al., Nucl. Phys. A 561 (1993) 298.

[25] W. Benenson, D. J. Morrissey, W. A. Friedman, Ann. Rev. Nucl. Part. Sci. 44 (1994) 27, and references therein. C. K. Gelbke, Nucl.Phys. A 495 (1989) 27c; J. Pochodzalla et al., Phys.Rev. C 35 (1987) 1695; H. Xi et al., Nucl.Phys. A 552 (1993) 281; F. Zhu et al., Phys.Rev. C 52 (1992) 784.

[26] S. Albergo, S. Costa, E. Costanzo, A. Rubbino, Nuovo Cimento A 89 (1985) 1.

[27] W. A. Friedman, Phys.Rev. C 42 (1990) 667.

[28] L. Phair et al., Nucl.Phys. A 564 (1993) 453; W. C. Hsi et al., Phys.Rev.Lett. 73 (1994) 3367; S. C. Jeong et al., Phys.Rev.Lett. 72 (1994) 3468.

[29] H. Xi, W. G. Lynch, M. B. Tsang, W. A. Friedman, MSUNSCL preprint 1040 (1996).

[30] Z. Majka et al., Phys.Rev. C, submitted.

[31] M. Assenard and the INDRA collaboration, contribution to this conference.

[32] A. Chbihi et al., preprint GANIL (1995) 24.